ISBN: 978-3-95450-223-3 ISSN: 2673-7000 doi:10.18429/JACoW-NAPAC2019-TUZBB5

TRANSVERSE ION BEAM EMITTANCE GROWTH DUE TO LOW FREQUENCY INSTABILITIES IN MICROWAVE ION SOURCE PLASMA

C. Mallick[1, 2, †] M. Bandyopadhyay[1,2,3] and R.K. Kumar[1,2]
[1]Institute for Plasma Research (IPR), Gandhinagar, Gujarat, India
[2]Homi Bhabha National Institute (HBNI), Anushaktinagar, Mumbai, Maharashtra, India
[3]ITER-India, Institute for Plasma Research, Gandhinagar, Gujarat, India

Abstract

The microwave ion source plasma is accompanied by the generation of low frequency (LF) plasma instabilities (PI). The signature of it can also be visible in high current ion beam required for any accelerator applications. These LFs may affect the profile of the ion beam in transverse phase-space. These issues are investigated by measuring the emittance of beam. The beam oscillations are extracted from the transverse emittance data by carrying out Fast Fourier Transform (FFT) analysis of it. The PI frequencies are identified in the measured electromagnetic emission from the plasma by a microwave spectrum analyzer, in which these frequencies appeared as sidebands around the launched frequency 2.45 GHz. The PI components are also visible in the FFT spectra of an Allison beam emittance scanner data. The oscillations in the extracted beam may be generated because of the plasma perturbations (or instabilities) by drift wave frequency and due to the presence multiple closely-spaced cavity modes around 2.45 GHz. The measured beam emittance (rms-normalized) in horizontal and vertical phase-space varies from 0.002-0.098 π mm mrad and 0.004-0.23 π mm mrad respectively due to increase of MW power from 250 W-700 W. The PI induced beam oscillation may be the reason behind such broad transverse emittance growth.

INTRODUCTION

Maintaining a least emittance growth of the ion beam during its transport through a low energy beam (LEBT) transport system is essential to minimize the beam loss at the mouth of an accelerator. One of the initial starting sources of beam emittance growth may hails from the plasma perturbations of drift wave frequency range, present in the ion source itself. In addition, multiple close-frequency heating (MCFH) in the Electron Cyclotron Resonance (ECR) ion source can also perturb plasma that may cause more growth in the beam emittance compared to the previous case. The MCFH is a well-established method in terms of production of highly intense and stable higher-charge-state ion beams [1-3]. This type of heating is also useful in mitigating the plasma instability [4]. The dynamics of perturbed plasma particles (electron and ion) is two-dimensional in their velocity phase-space if the frequency gap between the different combinations of heating frequency pairs is more than 1 GHz [4]. Under this condition, the particles' diffusion becomes similar to the case of single frequency heating (SFH). Hence, the MFH in which the frequency differences are in the GHz range shows no significant impacts on the ion beam emittance [5]. On the other hand, in the case of MCFH, (frequency gap ~ few 100's of MHz), the plasma may be perturbed significantly mainly in the sheath region. The dynamics of perturbed plasma particles is described by its diffusion under four-dimensional velocity phase-space [4 and 6]. As a result, the perturbed particles' distribution in four dimensional phase-spaces may affect the transverse beam emittance. In case of SFH, the electron's diffusion in velocity phase-space is remained as two dimensional in velocity phase-space [4]. It was demonstrated experimentally that two close-frequency heating (TCFH) is capable of suppressing the plasma kinetic instabilities and improving the confinement time of plasma electrons [4-7]. Recently, a less intense but stable ion beam compared to the SFH was produced experimentally [4 and 7] using MFH. The study related to the dependence of ion beam emittance on the instabilities generated due to the plasma perturbations is still relatively unexplored in the research community. In the present study, the impacts of plasma instabilities on the ion beam oscillations and its transverse emittance growth is investigated.

The present MW ion source supports multiple cavity dependent resonant modes [8]. Some of them are excited in plasma having equivalent intensity with respect to launched MW 2.45 GHz. The presence of these multiple close frequency modes around the launched one in this plasma filled cavity may perturb the MW E-field distributions due to the shifting of MW E-fields corresponding to one mode to another mode or vice versa [9]. This can yield a different steady state features of plasma. The physics associated with multiple closely-spaced excited modes may be considered as similar to the case of MCFH in an ion source. During the propagation of those excited MW modes, a fraction of every MW's energy is reflected off their corresponding critical plasma density layers. The reflected MW mode may change its polarization and convert into another mode near a mode conversion layer. The presence of excited closely-spaced MW modes may also perturb the E-field profiles within the sheath region. It is well known through analytics and experiments that the existence of strong inhomogeneous electric field within the plasma-sheath layer is associated

---

[†] Chinmoy.mallick@ipr.res.in

with the high tail of fast-electrons layer within the sheath [10]. In this paper, experiments are done to study the effects of plasma instabilities on the beam emittance growth and its oscillations. A correlation between plasma instabilities and beam oscillations which occur in the range from few hundreds of kHz to 1.3 MHz range is found. The MHz range beam oscillations which are argued to be originated from the generation of that strong inhomogeneous E-field within the plasma sheath are demonstrated through MW-plasma simulations and analytical calculations.

EXPERIMENTAL METHODS

In experiment, two types of diagnostics are used (Fig. 1) for the purpose of simultaneous measurement of transverse beam emittance and plasma instabilities. An Allison type emittance scanner is installed just behind the vacuum chamber to measure the ion beam emittance. The emittance scanner is placed at approximately 80 cm away from the plasma grid wall (or Boron nitride plate).

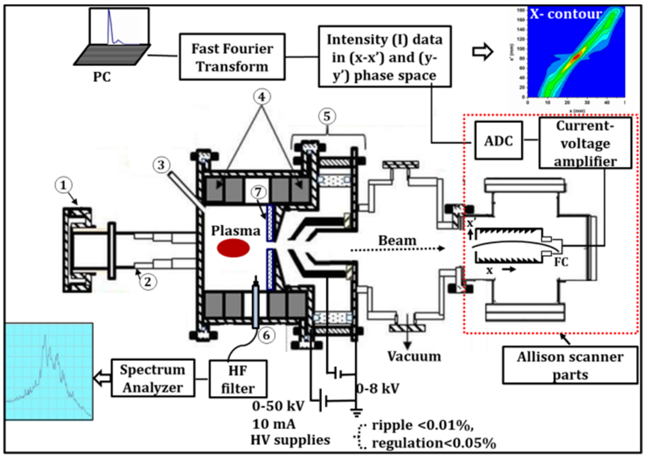

Figure 1: Schematic view of MDIS plasma and its beam emittance diagnostics setup. ① Vacuum window; ② Ridge guide;③ Gas inlet;④ Ring magnets pairs;⑤ ion extraction grids;⑥ RF probe;⑦ Boron nitride (BN) plate.

The intensity data is taken at a fixed particular voltage applied across the deflecting plates (or a fixed transversal point) of the emittance scanner. In order to record more number of beam intensity data, the velocity of the horizontal and vertical scanner heads were kept at minimum value (~ 10*nm/s*).

The beam oscillation frequencies are extracted from the beam intensity data taken at a particular position by performing the Fast Fourier Transform analysis. The number (N) of data points used in the FFT varies from 200-300. Hence, the frequency resolution (F_s/N) varies from ~3.3 kHz- 5 kHz for a sampling rate of 1 MHz. The inbuilt current-voltage amplifier (Trek Model PZD700A) within the Allison scanner has some interesting features, such as bandwidth (>200 kHz) [11] and sampling rate (1 MHz) [11]. Generally, the small signal bandwidth of the amplifier lies typically in the range of 350 kHz [11].

The plasma instability is investigated from the measured EM frequency emission of the MW plasma. The EM emission spectra are captured by a RF probe immersed in the plasma through a vacuum feed-through and connected to a high frequency band-pass filter. The spectrum is displayed on a microwave spectrum analyzer (model:FSH8, make: ROHDE & SCHWARZ, band: 100 Hz-8 GHz). The type of plasma instability is identified from the sidebands appearing around the different MW cavity mode frequencies in the emission spectra.

EXPERIMENTAL RESULTS

Beam

Figure 2 (a-f) shows the phase-space distribution of ion beam particles' intensity in *x* and *y*-planes for three different injected microwave powers. Below 250 W, it is observed (not shown in Fig. 2) experimentally that transverse emittance variation in the *x-x'* and *y-y'*-planes is small. The rms-normalized value of the emittance is calculated based on the equations given in [12]. In the calculation, 90% of beam fraction is included from the distribution shown in Fig. 2 (a-f). Fig. 2 (a-f) shows transverse emittance is increased by 2-4 times with increase in power. The rms-normalized emittance $\varepsilon_x^{rms-norm}$ and $\varepsilon_y^{rms-norm}$ ranges from 0.002-0.098 π -mm-mrad and 0.004-0.23 π -mm-mrad respectively. It is seen in Fig. 2(g) that the emittance increases nonlinearly with power. Fig. 2(h) gives the beam oscillations at 400 W. Fig. 2 (h) shows the corresponding beam oscillation frequencies obtained by taking the FFT of the transverse ion beam emittance data. Fig. 2 (h) shows two frequency peaks (i.e., ~ 476-873 kHz and ~1.3 MHz) of oscillations in the ion beam. The intensity of kHz range oscillations is much more than the MHz oscillations. The transverse ion beam oscillations in the range of ion wave frequencies are seen in both planes ($x -$ axis and $-$axis) of the beam emittance phase-space. However, it is observed experimentally that the influence of plasma perturbations on the $\mathrm{x} -$ plane oscillations of ion beam is not as significant as in the case of $\mathrm{y} -$ plane oscillations. Hence, the transverse emittance spread on $y -$ plane of ion beam is showing more in Fig. 2 (a-e) as compared to the $x -$ plane emittance.

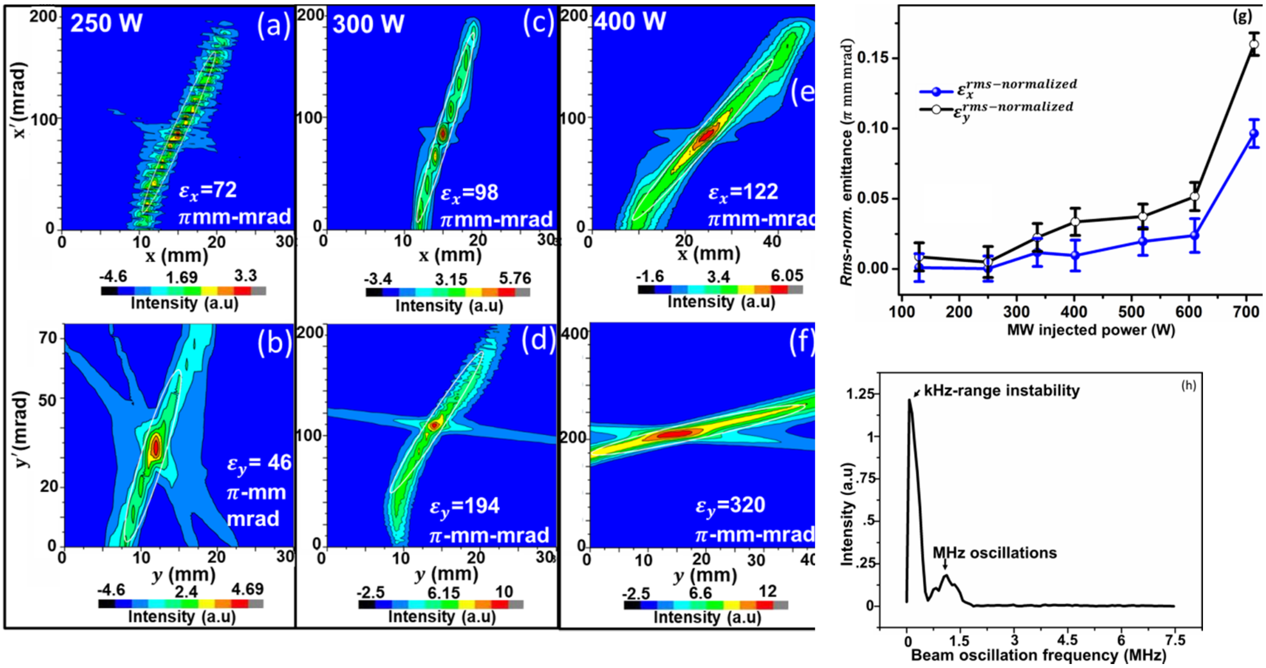

Figure 2 (a-f): Phase-space distributions of ion beam particles of different intensities in the x and y-planes (g) Transverse rms-normalized emittance (x and y-plane) growth with increase in MW power. (h) Beam oscillations of kHz and MHz range shows different amplitudes at their corresponding frequency range respectively.

Plasma

Figure 3 shows the electromagnetic frequency emission spectra from plasma at 400 W. It shows frequency peaks of three excited cavity resonant modes (i.e., #1, #2 and #3) in presence of plasma.

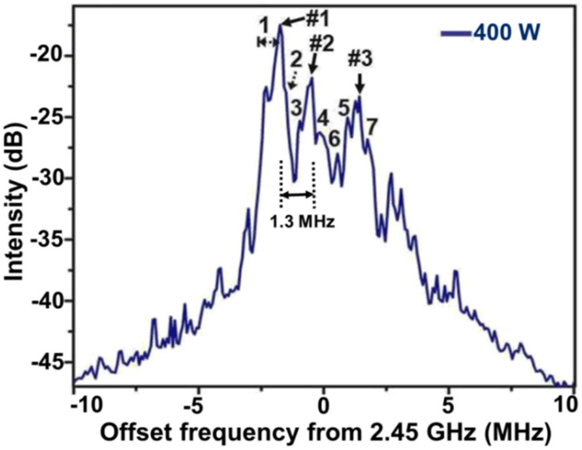

Figure 3: Electromagnetic frequency emission from plasma. Sideband peaks are numbered as 1 (555 kHz), 2 (238 kHz), 3 (476 kHz), 4 (317 kHz), 5 (397 kHz), 6 (873 kHz) and 7 (348 kHz).

The every peak is spaced apart from each other by a fixed sideband frequency of ~1.3 MHz. Additionally, each cavity mode peak is associated with side peaks (named as, 1,2,3… *etc.*) with different sideband values ranging from 238 kHz to 873 kHz. After comparing, Fig. 2 (h) and Fig. 3, it can be visualized that the kHz-range (476-873 kHz) beam oscillations belongs to the frequency range similar to the perturbed plasma wave's frequency (300-600 kHz) range which are originated from the drift instability [8, 13]. The E×B drift instability frequency of the plasma is already verified from the measured plasma potential gradient and simulated electric field distribution in ref.8. The effect of drift wave instabillities has not significantly impacted the transverse beam emittance. In Fig. 2 (h), beam oscillations contains two frequency components which are 476 - 873 kHz and 1.3 MHz range. The amplitude of MHz range beam oscillations is very low compared to kHz-range. It is observed from the repeated measurement that the beam emittance is enhanced by 2-4 times when the MHz range beam oscillations are present in the beam.

MW-PLASMA SIMULATION

In search of possible sources of those kHz and MHz-range beam oscillations, MW-plasma simulation is performed in COMSOL Multiphysics software under similar experimental system configuration and operating environment.The simulated electric field profile (see Fig. 4) show strong inhomogeneous layers within the plasma sheath region.The scale size of inhomogeneity is ~4-8 mm longitudinally and the gap between two inhomogeneous packet is less than 0.1 mm.The presence of strong inhomogeneous E-field in the plasma sheath may be responsible for generating fast (high energy) electrons through volume electron heating phenomenon as demonstrated in [14, 15] and following the relations [14, 15]: $\mathrm{F}_{\mathrm{avg}} \propto \nabla(\mathrm{E}^2)_{\mathrm{avg}}$. Here $\mathrm{F}_{\mathrm{avg}}$ is the force exerted on the electrons by the high frequency (HF) MW E-field. The fast electrons production can happen following this relation provided that frequency of MW is very high compared to local plasma resonance frequency of the sheath region [14, 15]. Now, as the two inhomogeneous layers are very close to each other along the magnetic field gradient line in such a mirror-type B-field configuration, the electrons/ions' energy are enhanced hugely in both the parallel and perpendicular direction with respect to B-field respectively [4, 6, and 16]. Hence, the plasma ions' motion is perturbed due to the presence of strong inhomogeneous E-field layers. To find out the frequency of this perturbed plasma motion, analytical calculation is performed in case of extraordinary (*X*) type MW.

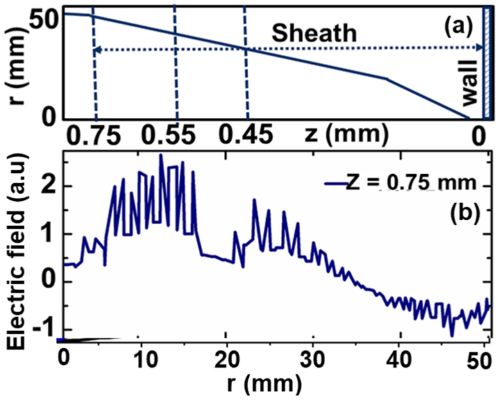

Figure 4: (a) Plasma sheath near BN-plate (b) Strong inhomogeneous E-field layers within plasma sheath.

THEORETICAL ANALYSIS

For *X*-mode MW, the set of Maxwell's equations can be simplified to the modified Bessel's differential equations in terms of the axial component of wave magnetic field, H_z [16, 17]. The solution to this differential equation in the plasma region and the plasma-wall interface (or the sheath region) region is as follows [17]:

$$H_z = A_1\, I_m(Kr);$$
$$H_z = A_2[\, J_m(\kappa r)N'_m(\kappa R) - J'_m(\kappa R)N_m(\kappa r)].$$

Here $K^2 = (\omega/c)^2(\varepsilon_2^2 - \varepsilon_1^2)\varepsilon_1^{-1}$ and $\kappa^2 = (\omega/c)^2\,\varepsilon_s$. Where A_i (i = 1 and 2), K^{-1}, $J_m(\kappa r)$ and $N_m(\kappa r)$, ε_i(i = 1 and 2), ε_s, ω and c are real constants, penetration depth of X-mode MW into plasma, Bessel function of 1st kind, Bessel function of 2nd kind, two components of permittivity present in this MW plasma cavity (where $\varepsilon_1 = 1 - \Omega_\alpha^2/(\omega^2 - \omega_\alpha^2)$ and $\varepsilon_2 = -\Omega_\alpha^2\omega_\alpha/\omega(\omega^2 - \omega_\alpha^2)$)[14], permittivity of sheath, wave frequency, speed of light, respectively. Here, Ω_α and ω_α are the plasma and cyclotron frequencies of plasma particle species α (α = i for ion and e for electrons).

The condition $K^2 > 0$ determines the possible frequency ranges within which the *X*-mode propagates at the interface region of plasma-boundary wall. The solution to this inequality gives two frequency ranges, i.e. low (LF) and high frequency (HF) waves whose ranges are $\omega_{LF} < \omega < |\omega_e|$ and $|\omega_e| < \omega < \omega_1 - |\omega_e|$, respectively. Here $\omega_{LF} = [\Omega_i^{-2} + (\omega_i|\omega_e|)^{-1}]^{-1/2}$ and $\omega_1 = 0.5\omega_e + [\Omega_e^2 + 0.25\,\omega_e^2]^{1/2}$.

For the simulated plasma parameters (see Fig. 5a), n_i= 5.5× 10^{15} m^{-3} and $B = 0.23\,T$ near the plasma-wall boundary regions, the wave frequency are estimated from the above relation to be ω_{lh} = ~1.3 MHz. The existence of this range of frequency within the plasma sheath may arise from the perturbations of plasma ion's motion due to the presence of strong inhomogeneous E-field layers as discussed above.

The frequency of the waves which propagates at the interface region of plasma column and plasma sheath depends on the plasma column radius and sheath thickness [16]. For the 'zeroth radial mode (l = 1)' [18] and azimuthal mode number, m = 1, the eigen-frequency of the HF wave propagating in the interface zone is given below following the relation written in [16]:

$$\omega \approx {}^{\pi c}\!/_{\sqrt{\varepsilon_s}(R-r)}\,[1 - \frac{\varepsilon_2 c^2}{\varepsilon_1\Omega_e^2 r(R-r)}].$$

Here *(R-r)*, *r* and *R* are sheath thickness, inner and outer radius of plasma sheath respectively.

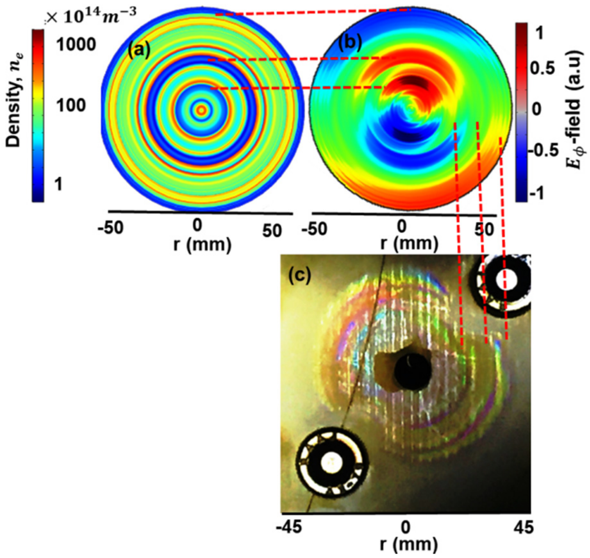

Figure 5: (a) Simulation results showing discrete density layers along the radial line within the plasma sheath. Blue colored plasma rings denote minimum plasma density regions. Red dot lines denotes different surfaces exist in radial direction. (b) Surface plot of strong inhomogeneous E_ϕ-field component. (c) Camera snapshot of inside view of experimental cavity shows footprint of three layers of fast electrons propagating within the plasma sheath mainly in the ϕ-direction.

Obtaining the simulated data, i.e., for the plasma column radius and thickness of plasma column to wall of 44 mm and 1.62 mm respectively, B = 0.26 T, ε_s=1, and n_e= 5.5× 10^{15} m^{-3} at the plasma sheath region, the high frequency wave is estimated to be 2.453 GHz which lie within the measured frequency emission range as shown in Fig. 3.

VALIDATION WITH EXPERIMENT

Figure 5 (a) and (b) show the simulated 2D plots (r-ϕ variation) of the plasma density and E-field respectively within the plasma-BN plate interface or the plasma sheath region. Fig. 5(a) show discrete density layers formed within the plasma sheath in the radial direction. Three distinct but closely-spaced layers of strong inhomogeneous E-field is also shown accordingly in Fig. 5 (b) at the same interface location. This strong inhomogeneous E-field may produce high energy tail of electrons as per the relation, $\mathrm{F_{avg}} \propto \nabla(\mathrm{E}^2)_{\mathrm{avg}}$, discussed above. The fast electrons' layers present within the sheath location makes the plasma density profile discrete in nature in the radial direction following electric field profile. Fig. 5(c) shows the experimental footprint of fast electrons' layers within the plasma sheath. The propagating fast electrons are driven by mainly the azimuthal component of E-field (E_ϕ). The experimental footprint of fast electrons on the BN plate is caused due to the interaction of fast electrons with the BN plate plasma facing surface.

SUMMARY

The transverse ion beam emittance and the plasma stimulated electromagnetic frequency emission are measured simultaneously using two diagnostic instruments (Allison scanner and microwave Spectrum Analyzer respectively) at different input microwave powers. The emittance increases by 2-4 times when the instabilities related to the plasma perturbations in the kHz and MHz frequency range are present in the plasma. However, the effect of kHz range drift wave instability on beam emittance is not as significant as the case of 1.3MHz plasma perturbations due to the presence of multiple cavity modes having close frequencies in plasma. A correlation between the plasma instability frequency and beam oscillations frequency is obtained. Evidence of experimental results supported by the simulation envisages that the existence of multiple excited cavity modes may yield strong inhomogeneous E-field layers within the plasma sheath and correspondingly a force is generated which primarily accelerates the electron to reach high energy. As a result of that, plasma ions' motion may be perturbed in the transverse direction with respect to the external B-field in MHz frequency range within the thin layer of sheath and correspondingly MHz beam oscillation arises.

REFERENCE

[1] Z. Q. Xie, and C. M. Lyneis, “Two-frequency plasma heating in a high charge state electron cyclotron resonance ion source,” *Rev. Sci. Instrum.*, vol. 66, p. 4218, 1995. `doi.org/10.1063/1.1145372`

[2] M. Sakildien *et al.*, “Studying the double-frequency heating mode in ECRIS plasma using Kα diagnostics,” *AIP Conference Proceedings*, vol. 2011, p. 040011, 2018.

[3] A. Kitagawa *et al.*, “Two-frequency Heating Technique for Stable ECR Plasma”, in *Proc. 20th Int. Workshop on ECR Ion Sources (ECRIS'12)*, Sydney, Australia, Sep. 2012, paper TUXO03, pp. 10-12.

[4] Eugenia Naselli *et al., Plasma Sources Sci. Technol.*, in press `https://doi.org/10.1088/1361-6595/ab32f9`.

[5] Olli Tarvainen *et al.*, “Studies of electron cyclotron resonance ion source plasma physics,” thesis, Jyväskylä, Finland, December, 2005 (ISBN-978-951-39-3165-0).

[6] J.E. Howard *et al.*, “Four-dimensional mapping model for two-frequency electron cyclotron resonance heating,” *Physica D*, vol. 20, pp. 259-284, 1986.

[7] R. Rácz *et al.,* “Effect of the two-close-frequency heating to the extracted ion beam and to the X-ray flux emitted by the ECR plasma,” *JINST*, vol. 13, p. C12012, 2018.

[8] C. Mallick, M. Bandyopadhyay, and R. Kumar, “Plasma characterization of a microwave discharge ion source with mirror magnetic field configuration,” *Rev. Sci. Instrum.*, vol. 89, p. 125112, 2018.

[9] R. Geller, *Electron Cyclotron Resonance Ion Sources and ECR Plasmas*, Bristol: Institute of Physics, 1996.

[10] Yu. M. Aliev, V. Yu. Bychenkov, A. V. Maximov and H. Schluter, “Plasma Sources Science and Technology High energy electron generation in surface-wave-produced plasmas,” *Plasma Sources Sci. Technol.*, vol. 1, pp. 126-131, 1992.

[11] R. D’Arcy *et al.*, “Characterisation of the PXIE Allison-type emittance scanner,” *Nucl. Instrum. Methods Phys. Res. A,* vol. 815, pp. 7-17, 2016.

[12] A. J. Mendez and Y. Liu, “Extraction simulations and emittance measurements of a Holifield Radioactive Ion Beam Facility electron beam plasma source for radioactive ion beams,” *Rev. Sci. Instrum.,* vol. 81, p. 02B712, 2010. `doi.org/10.1063/1.3290859`

[13] S. Kumar *et al.,* “Experimental investigation of plasma instabilities by Fourier analysis in an electron cyclotron resonance ion source,” *Phys. Rev. Accel. and Beams*, vol. 21, p. 093402, 2018.

[14] G. A. Askar’yan, “Cerenkov Radiation and Transition Radiation from Electromagnetic Waves,” *Sov. Phys. JETP*, vol. 15, p. 943, 1962.

[15] G. A. Askar’yan *et al.*, “Emission of Radio Waves Upon Modulation of an Intense Beam of Light in a Medium,” *Sov. Phys. JETP* vol. 18, p. 441, 1964.

[16] I. O. Girka, V. M. Kondratenko, and M. Thumm, “Higher radial modes of azimuthal surface waves in magnetoactive cylindrical plasma waveguides,” *J. Plasma Phys.*, vol. 84, p. 905840603, 2018. `doi:10.1017/S0022377818001101`

[17] B Jazi and H Mehdian, “Dispersion relation of azimuthal electromagnetic surface waves on a magnetized plasma column in a dielectric lined slow-wave waveguide*,” Plasma Phys. Control. Fusion,* vol. 46, pp. 507-518, 2004.

[18] V. O. Girka *et al.*, *Soviet Journal of Communications Technology and Electronics*, vol. 33, pp. 37-41, 1988.